Available online at www.sciencedirect.com
ScienceDirect
Biochemical and Biophysical Research Communications 353 (2007) 18–25
BBRC
www.elsevier.com/locate/ybbrc

Differential regulation of splicing, localization and stability of mammalian ARD1^{235} and ARD1^{225} isoforms

Kwang-Hoon Chun, Seung-Ju Cho, Joon-Seok Choi, Se-Hee Kim, Kyu-Won Kim *, Seung-Ki Lee *

Division of Pharmaceutical Biosciences, College of Pharmacy, The Research Institute for Pharmaceutical Sciences, Seoul National University, Seoul 151-742, Republic of Korea

Received 3 November 2006
Available online 5 December 2006

Abstract

ARD1 protein is a mammalian gene product homologous to a yeast Ard1p (Arrest defective 1 protein) acetyltransferase. Although two alternative splicing products of ARD1, ARD1^{235} and ARD1^{225}, were reported in mouse, only ARD1^{235} orthologue was reported in humans. Here we show that ARD1^{225} is not expressed in humans, suggesting that factors regulating alternative splicing of ARD1 may have evolved differently between species. In human cells, hARD1^{235} is shown to be present in both nucleus and cytoplasm. However, in mouse cells, mARD1^{235} and mARD1^{225} proteins are localized to the nucleus and cytoplasm, respectively. Moreover, during apoptosis, ARD1^{235} and ARD1^{225} isoforms are destabilized by different mechanisms in a species-specific manner and dependent on destabilizing reagents. These results indicate that ARD1^{235} and ARD1^{225} isoforms may have different activities and function in different subcellular compartments of mammalian cells.

Keywords: ARD1; HIF-1α; Alternative splicing; Apoptosis; Acetyltransferase

Protein acetylation is an important post-translational modification critical for both normal cell function and oncogenesis [1,2]. ARD1 was first described in *Saccharomyces cerevisiae* [3], and the human and mouse ARD1^{235} isoforms are reported to form a stable complex with the mammalian homologue of NAT1p [4,5]. The mouse ARD1^{225} isoform is known to promote proteasomal degradation of HIF-1α [6]. At present, the existence of ARD1^{235} isoform in human and mouse cells has been confirmed by examining nucleotide and protein databases and the literature [4,5]. However, ARD1^{225} isoform has only been reported in mouse cells [6,7], and it is unclear whether ARD1^{225} is expressed in human cells or not.

It was reported that hARD1^{235} is localized to the nucleus and cytoplasm [4] or predominantly cytoplasm [8] in HeLa cells. Ectopically expressed mouse ARD1^{235} and ARD1^{225} have been reported to be localized mainly to the cytoplasm in rat kidney fibroblast cells (NRK-49F) [5] and HT1080 human fibrosarcoma cells [6], respectively.

Here, we demonstrate that ARD1^{225} is an alternative splicing isoform specific to mouse. Also, we show that ARD1^{235} and ARD1^{225} display unique subcellular localizations and exhibit different stabilities depending on cell type and apoptotic stimuli. These results indicate that humans and mouse might develop different mechanisms for the synthesis of ARD1 products and, furthermore, that ARD1^{225} isoform may function differently from ARD1^{235} in mammalian cells.

Materials and methods

Cell culture. HeLa human cervical adenocarcinoma cells, 293T human renal epithelial cells, HT1080 human fibrosarcoma cells, MBEC mouse microvascular brain endothelial cells and NIH-3T3 mouse embryonic fibroblasts were cultured in Dulbecco's modified Eagle's medium

* Corresponding authors. Fax: +82 2 889 0751.
E-mail addresses: qwonkim@plaza.snu.ac.kr (K.-W. Kim), sklcrs@plaza.snu.ac.kr (S.-K. Lee).

0006-291X/$ - see front matter © 2006 Elsevier Inc. All rights reserved.
doi:10.1016/j.bbrc.2006.11.131

(DMEM, Gibco-BRL Life Technologies) supplemented with 10% fetal bovine serum (FBS) in a humidified incubator with 5% CO_2 at 37 °C. THP-1 human monocytic leukemia cells and MCF-7 human breast cancer cells were cultured in RPMI1640 medium (Gibco-BRL Life Technologies) with 10% fetal calf serum (FCS). Raw264.7 mouse monocytes were cultured in RAW 264.7 growth medium 1 (RAWGM1). JB6 mouse neonatal BALB/c epidermal cells were cultured in minimum essential medium (MEM) with 5% FBS. CCE mouse embryonic stem cells were maintained on gelatin-coated dishes without feeders in knockout-DMEM with 15% defined serum replacement (Knockout SR™, Invitrogen), 100 U/ml leukemia inhibitory factor (ESGRO, Chemicon), 1 mM L-glutamine, 0.1 mM β-mercaptoethanol and 1% nonessential amino acids.

Primer design for RT-PCR analysis. To identify ARD1 cDNAs, four sets of PCR primers were designed from human and mouse ARD1 cDNAs (GenBank Accession No. NM_003491 for hARD1^{235}, NM_019870 for mARD1^{235} and BC027219 for mARD1^{225}) as described in Table 1.

RNA extraction and cDNA synthesis. For RT-PCR experiments, total RNA was extracted from cell lines using Trizol reagent (Gibco-BRL Life Technologies). cDNA was synthesized by incubating RNA with 200 units of MMLV-RT (Promega) and 500 ng of oligo-$(dT)_{16}$ primers in 20 μl of reverse transcription buffer provided by manufacturer with 0.45 mM dNTP at 42 °C for 50 min and then 70 °C for 15 min.

Polymerase chain reaction. cDNA pools were used as templates for PCR using P1, P2, P3 and P4 primers for ARD1 in a total volume of 50 μl using Peltier Thermal Cycler-100 (MJ Research). Briefly, 1 μl of aliquots of cDNA, PCR buffer provided by manufacturer, 250 μM each of dNTPs, 2 pmol of a set of PCR primers and 1 unit of Han-Pfu polymerase (Genenmed Inc.). PCR was performed with an initial denaturation step of 4 min at 95 °C, followed by 95 °C for 1 min, 45 °C for 40 s, 72 °C for 100 s for 35 cycles and a final extension for 10 min at 72 °C. PCR products were analyzed by electrophoresis on agarose gels.

Alignment of ESTs and genome sequence. To analyze exon–intron junctions, human and mouse ARD1 cDNA sequences were aligned with genomic DNA sequence (GenBank Accession No. NT_025965 for human ARD1; NT_039706 for mouse) using MAP Viewer of the NCBI website (http://www.ncbi.nlm.nih.gov/mapview). Homology analyses of mARD1^{235} and mARD1^{225} proteins were performed by a BLAST search (http://www.ncbi.nlm.nih.gov/blast). Analysis of the ARD1 genomic sequence was performed using the UCSC genome browser (http://genome.ucsc.edu).

Western blotting. Cell lysates were resolved by 12% SDS polyacrylamide gel electrophoresis (SDS–PAGE), and electro-transferred onto PVDF membrane (Gelman). The membrane was blocked with 5% non-fat milk (Carnation®, Glendale) in PBS and probed with rabbit polyclonal anti-ARD1 antibody (1:1000), mouse monoclonal anti-GFP antibody (1:1000; Santa Cruz Biotechnology) and mouse monoclonal anti-α-tubulin (1:2000; Santa Cruz Biotechnology). Anti-ARD1 antibody was produced by Dinano (Korea) using an immunogen corresponding to amino acids 1–20 of ARD1, which is identical in human and mouse. Horseradish peroxidase-conjugated anti-rabbit and anti-mouse IgG were from Perkin-Elmer. Immunoreactivity was detected with WEST-ZOL plus Western blotting detection reagents (Intron Biotechnology).

Confocal microscopy for visualization of endogenous ARD1. Cultured cells on coverslips were incubated in blocking buffer (0.5% BSA/2% CAS block solution (Zymed)/PBS) for 1 h at room temperature and then with anti-ARD1 antibody (1:100) in blocking buffer overnight at 4 °C. Cells were washed three times for 5 min each in 0.05% BSA/PBS and then incubated with FITC-labeled secondary antibody (Santa Cruz Biotechnology) in blocking buffer for 60 min at 37 °C. For nuclear staining, cells were washed in 0.05% BSA/PBS for 10 min once and for 5 min twice and then incubated with 50 μg/ml propidium iodide (PI, Sigma) and 100 μg RNaseA (Sigma) for 30 min at 37 °C. Cells were washed three times with 0.5% BSA/PBS and mounted with GEL/MOUNT (Biomeda). Cells were visualized and images acquired on a laser scanning confocal microscope (Leica).

Cell fractionation. Cultured cells were washed with PBS and then Dounce-homogenized (35 strokes) in homogenization buffer (10 mM HEPES, pH 7.4, 10 mM KCl, 2 mM $MgCl_2$, 5 mM EGTA, 40 mM β-glycerophosphate, 1 mM dithiothreitol, 30% sucrose and 0.1 mM phenylmethylsulfonyl fluoride) and centrifuged at 4 °C for 20 min at 830*g*. For the cytosolic fraction, supernatants were transferred to Eppendorf tubes and re-centrifuged at 4 °C for 90 min at 15,000 rpm. For nuclear extracts the nuclear pellet was washed with PBS and resuspended with IP buffer (20 mM Tris, pH 7.5, 0.5% Triton X-100, 2 mM $MgCl_2$, 0.1 mM phenylmethylsulfonyl fluoride, 50 mM β-glycerophosphate, 25 mM NaF, 1 mM EGTA, 1 mM dithiothreitol and 1 mM sodium orthovanadate), centrifuged for 30 min at 12,000 rpm at 4 °C and the supernatant isolated. Protein concentration was determined using the BCA assay. Proteins were analyzed by SDS–PAGE as described above.

Results

Expressions of ARD1 isoforms are differently regulated in human and mouse cells

Previously, ARD1^{235} was observed in human and mouse cells [4,5] and ARD1^{225} only in mouse [6]. ARD1^{235} and ARD1^{225} are identical from aa 1 to 157, which contains the conserved acetyltransferase motif region at aa 45–130, but differ at the C-terminus (Supplementary Fig. S1) [7]. Analysis of mouse ARD1 cDNA sequence shows that the mouse ARD1^{225} transcript has an additional 91 nucleotides starting at nt 472 relative to the start site, which results in a different reading frame and termination site (Fig. 1A). To determine whether ARD1^{235} and ARD1^{225} are expressed differently in human and mouse cells, we amplified ARD1 transcripts using RT-PCR from human (293T, MCF, THP-1 and HeLa) and mouse (CCE embryonic stem cells, NIH-3T3, MBEC and Raw) cell lines. Total RNA was extracted and cDNA synthesized. Four primer sets

Table 1
Design of primer sets for RT-PCR

Primer	Sequence (5′–3′)	Region (nt)
P1/P2/P4 sense	^{001}ATGAACATCCGCAATGCTAGG^{021}	1–21
P1 antisense	^{799}CTAGGAGGCAGAGTC^{785}	785–799
P2/P3 antisense	^{678}TCACGACAGGCCTCTCCTGAGCTCAAA^{652}	652–678
P3 sense	^{391}AGCGAAGTGGAGCCCAAATAC^{411}	391–411
P4 antisense	^{520}GGCCTAAGTCTCCAGACAGGAG^{498}	498–520

The sequences of P1/P2/P4 and P3 sense primers are conserved in human and mouse ARD1 genes and selected from either human (GenBank Accession No. NM_003491) or mouse (BC027219) ARD1 genes. Sense primers P1, 2 and 4 correspond to the region containing the start codon; the P3 sense primer corresponds to the region between the start codon and the region missing in ARD1^{235}. The P1 antisense primer corresponds to a region containing the mARD1^{235} stop codon; P2 and P3 antisense primers correspond to a region containing the mARD1^{225} stop codon. The P4 antisense primer corresponds to a region deleted in ARD1^{235}.

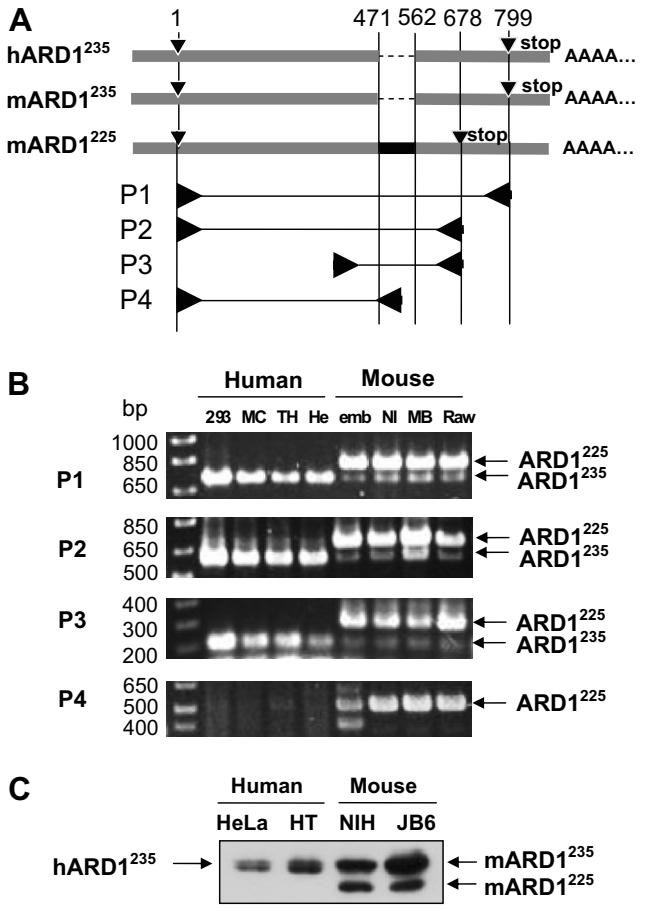

Fig. 1. Identification of ARD1 mRNA and proteins in human and mouse cells. (A) Alignment of ARD1 human and mouse ESTs using reference cDNA sequences and schematic structures of transcripts amplified by primer sets P1, P2, P3 and P4 in RT-PCR. The transcript ends are indicated by triangles. The region deleted in $ARD1^{235}$ is depicted as a dotted line. Numbers indicate nucleotide sequence. (B) Total RNA was extracted and a cDNA pool was prepared from human and mouse cell lines: 293T (293), MCF (MC), THP-1 (TH) and HeLa (He) human cell lines, and embryonic (emb), NIH-3T3 (NI), MBEC (MB) and Raw mouse cell lines. PCR was performed using P1, P2, P3 and P4 primers. (C) Cell lysates from HeLa and HT1080 (HT) human lines and NIH-3T3 (NIH) and JB6 mouse lines were prepared and subjected to SDS–PAGE. Immunoblotting was performed using an anti-ARD1 antibody.

named P1, P2, P3 and P4 from ARD1, as described in Table 1 and Fig. 1A, were used for PCR. As shown in Fig. 1B, when P1, P2 and P3 were used in PCR, two bands corresponding to the predicted size of $mARD1^{235}$ and $mARD1^{225}$ cDNAs were detected in mouse cell lines, while only one band corresponding to $hARD1^{235}$ was detected in human cell lines. A band corresponding to $ARD1^{225}$ was not detected in the human cell lines tested. Furthermore, when P4 primers were used, no band was detectable in human cell lines, supporting the idea that the region corresponding to nt 498–520 of $mARD1^{225}$ is not contained in $hARD1^{235}$ and $mARD1^{235}$ cDNAs. These results support that $ARD1^{235}$ is transcribed in human and mouse cells whereas $ARD1^{225}$ is not expressed in human cells. Next, the expression of ARD1 proteins was identified by Western blot analysis using an anti-ARD1 polyclonal antibody. Blots made from cell lysates showed two bands corresponding to $ARD1^{235}$ and $ARD1^{225}$ isoforms in NIH-3T3 and JB6 mouse cell lines, while only $ARD1^{235}$ isoform was seen in HeLa and HT1080 human cell lines (Fig. 1C). These results confirm that the $ARD1^{225}$ isoform is not expressed at the protein level in representative human cells while $ARD1^{235}$ protein is expressed in both human and mouse species.

$ARD1^{225}$ transcript is absent in human cells

To analyze differential expression of $ARD1^{225}$ in human and mouse cell lines, we aligned ESTs of human and mouse ARD1 genes using NM_003491 for $hARD1^{235}$, NM_019870 for $mARD1^{235}$, and BC027219 for $mARD1^{225}$ and analyzed the location of intron/exon boundaries using NCBI genome browser (http://ncbi.nlm.nih.gov/genome). Both $ARD1^{235}$ and $ARD1^{225}$ are composed of eight exons and $mARD1^{225}$ is spliced at an alternative 3′ splice site located 91 bp upstream of the 3′ splice site of exon VIIIa of $mARD1^{235}$ (Supplementary Fig. S2). The intron/exon boundaries are conserved as all introns have a GT and AG at their 5′ and 3′ ends, respectively (Supplementary Tables S1 and S2). To determine whether $hARD1^{225}$ transcripts could be generated from the human genome, we searched for alternative acceptor sites in the hARD1 genome (GenBank Accession No. NT_025965) that could be used to generate a putative $ARD1^{225}$ isoform. As shown in Fig. 2A, hARD1 genomic DNA shows no conserved acceptor site 91 bp upstream of the 3′ splice site of exon VIIIa, suggesting that the $ARD1^{225}$ transcript cannot be generated from the human genome. To determine whether the $ARD1^{225}$ isoform is expressed in other species, we searched for proteins orthologous to $ARD1^{235}$ and $ARD1^{225}$ by BLAST searches using aa 158–235 of $mARD1^{235}$ and aa 158–225 of $mARD1^{225}$. We defined proteins with an e-value $> 1e-10$ as orthologues. As shown in Table 2, orthologues corresponding to the $ARD1^{235}$ isoform were detected in human, mouse, rat, cow, dog, kangaroo, chimpanzee and frog, while that of the $ARD1^{225}$ was not seen in other species, confirming that $ARD1^{225}$ is unique to mouse. These findings suggest two possible mechanisms for the absence of $ARD1^{225}$ isoform in humans: one possibility is that human genome does not have a conserved 3′ splice site for exon VIIIb, thus, alternative splicing in exon VIIIb is not allowed, or another is that human genome has a conserved 3′ splice site for exon VIIIb in different region from mouse genome producing a kind of ARD1 isoform with a different size and codon usage. To determine these possibilities, we examined conservation of ARD1 exons in various genomes by aligning genomic sequence of hARD1 with 17 vertebrate genomes, including mammalian, amphibian, avian, and fish species and calculated a conservation score based on a phylogenetic hidden Markov model using the UCSC genome browser (http://genome.ucsc.edu) [9]. The data shows that most exons of

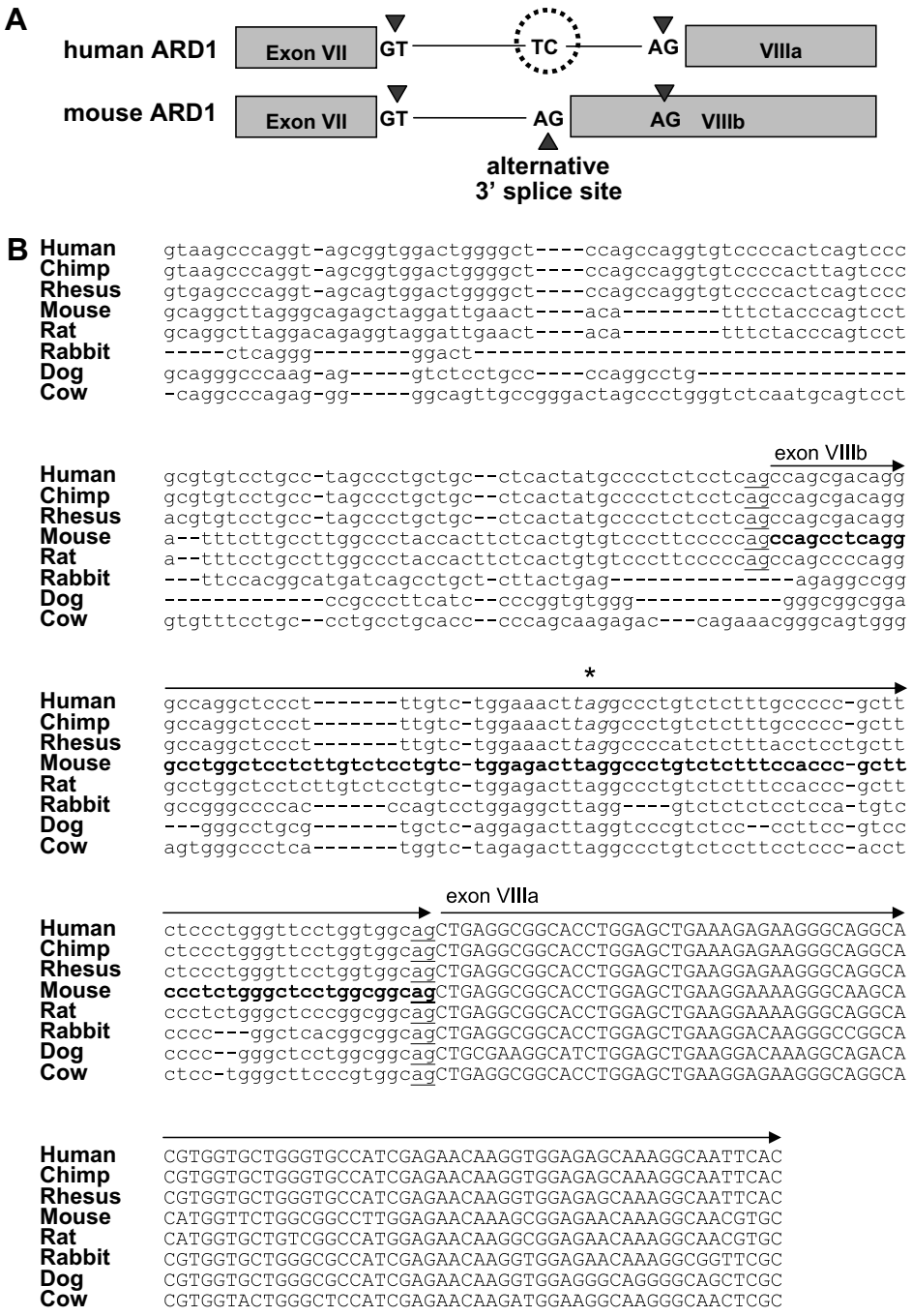

Fig. 2. The human genome does not have conserved GT-AG intron seen in mouse. (A) Intronic splice junction 5′ splice site and 3′ splice site upstream of exon VIIIa and VIIIb of the ARD1 gene are represented. The residues at intronic splice junction acceptor for virtual human ARD1^{225} are circled. (B) Multiple sequence alignment was conducted with ARD1 genomic sequences of human, chimpanzee, rhesus monkey, mouse, rat, rabbit, dog and cow. Nucleotides of exon VIIIa or mARD1 exon VIIIb are capitalized or in bold, respectively. A predicted stop codon in exon VIIIb of human, chimpanzee and rhesus monkey ARD1 is indicated by (*) and shown in italics. Conserved 3′ splice sites of exon VIIIa and VIIIb are underlined.

ARD1 genes are highly conserved among vertebrates, while, as expected, intronic regions are not (Supplementary Fig. S3). To evaluate the conservation of exon VIIIa and VIIIb in greater detail, we searched for 3′ splice sites by multiple alignment of human, chimpanzee, rhesus monkey, mouse, rat, rabbit, dog and cow genomic sequences (Fig. 2B). Such analysis showed that ARD1 exon VIIIa sequences are highly conserved over all species tested, while a putative 3′ splice site of exon VIIIb is not conserved in rabbit, dog and cow, indicating that an ARD1^{225} isoform may not be generated in these species. While the rat genomic sequence is highly homologous to that of the mouse in both the exon VIIIa and VIIIb regions, an ARD1^{225} protein has not been reported in rat as shown in Table 2. In

Table 2
BLAST search of ARD1 orthologues

Query	Species	e-value	Identity (%)	GI No.
aa 158–235 of mARD1^{235}	*Mus musculus*	5e − 36	100	51773477, 9845236, 12852343, 29242811, 23813733
	Rattus norvegicus	1e − 34	94	34881754
	Homo sapiens	4e − 31	88	10835057, 17939652, 12653085, 728880, 517485
	Pan troglodytes	4e − 31	88	55664728
	Bos taurus	7e − 31	87	76621207
	Canis familiaris	4e − 29	80	74008789, 74008787
	Xenopus laevis	3e − 14	55	28422354
	Macropus giganteus	6e − 14	62	68131953
	Xenopus tropicalis	8e − 14	52	51261910, 55926170
aa 158–225 of mARD1^{225}	*Mus musculus*	5e − 10	100	20071196, 26365817

We searched for proteins orthologous to ARD1^{235} and ARD1^{225} using the BLAST search of NCBI website (http://www.ncbi.nlm.nih.gov/blast) by submitting the unique sequence of each isoform: aa 158–235 ofmARD1^{235} and aa 158–225 ofmARD1^{225}. We judged proteins with an e-value > 1e − 10 to be orthologues.

addition, we found that human genomic sequence showed high conservation with both chimpanzee and rhesus monkey in both exons and introns. In humans, exon VIIIb has a consensus 3′ splice site sequence with a stretch of 9 pyrimidines, followed by T and C, and ending with AG (CCCCTCTCCTCAG). Thus, a predicted splice variant would introduce 84 additional nucleotides at the 5′ region of the human ARD1 exon VIIIa. However, unlike the case with mouse, the human gene shows different codon usage in the putative exon VIIIb conferring a stop codon (TAG) ahead of exon VIIIa (Fig. 2B), which would produce a truncated translation product (ARD1^{169}). The putative ARD1^{169} isoform was not detected either by RT-PCR or Western blotting and has not been reported by others.

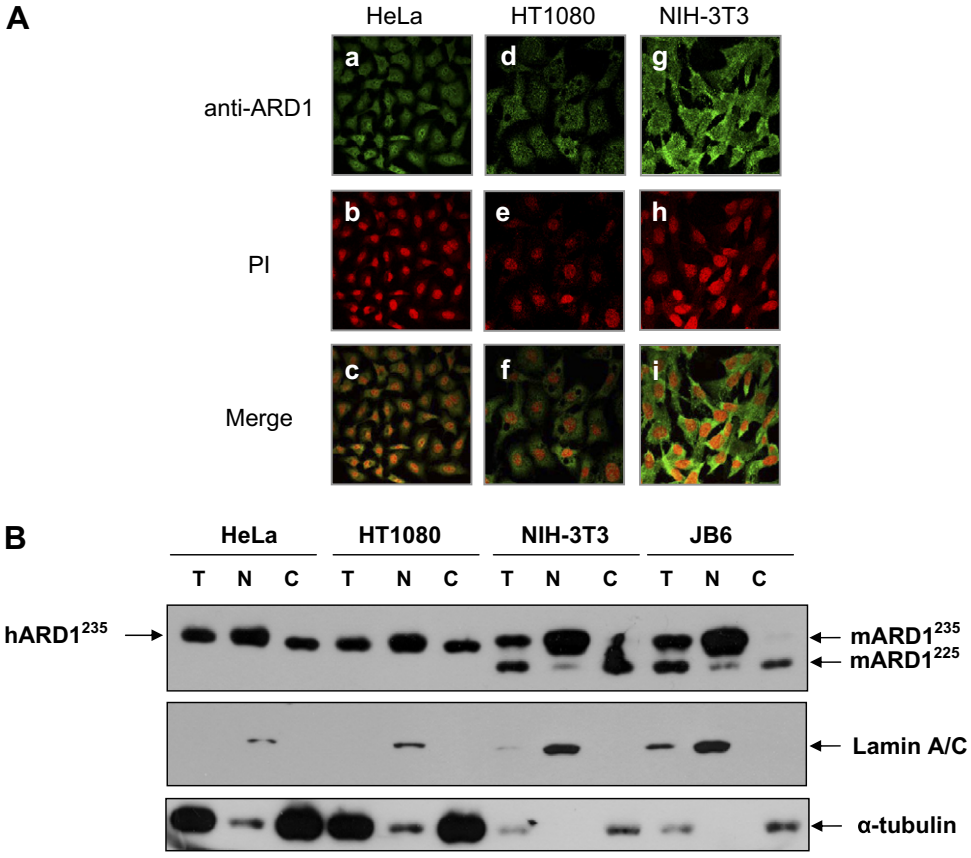

Fig. 3. Distribution of ARD1 proteins in human and mouse cells. (A) Cells were treated with anti-ARD1 antibody and then stained with an FITC-labeled secondary antibody and with PI to identify the nucleus. Cells were visualized by confocal microscopy. (B) Total cell lysate (T), nuclear (N) and cytosolic (C) enriched fractions were prepared from human (HeLa and HT1080) and mouse (NIH-3T3 and JB6) cell lines and analyzed by immunoblotting for ARD1 (upper panel). Lamin A/C was used as a nuclear marker (middle panel) and α-tubulin as a cytosolic marker (lower panel).

Altogether, these findings indicate that the expression of an ARD1^{225} isoform is not universal but is a species-specific event.

Subcellular localization of ARD1 proteins in human and mouse cell lines

Interestingly, ARD1^{225} is more hydrophobic than ARD1^{235} at the C-terminus, indicating that this region may confer a unique function to this isoform. Thus, we analyzed the subcellular localization of ARD1 isoforms in human (HeLa and HT1080) and mouse (NIH-3T3) cells by immunofluorescence confocal microscopy. Endogenous hARD1^{235} was evenly distributed in both nucleus and cytoplasm of HeLa and HT1080 cells (Fig. 3A). In contrast, endogenous mARD1 proteins were apparently more highly expressed in the cytoplasm than in the nucleus of NIH-3T3 cells (Fig. 3A). To confirm whether ARD1^{235} and ARD1^{225} are differentially localized, we fractionated lysates of human and mouse cell lines and then analyzed the subcellular distribution of ARD1 isoforms by Western blotting. Fig. 3B shows that hARD1^{235} protein is present in both nuclear and cytoplasmic compartments. In the case of mouse ARD1 isoforms, mARD1^{235} protein was distributed mainly in the nucleus while mARD1^{225} was primarily cytoplasmic. These results indicate that distribution of ARD1 proteins may be regulated by different mechanisms in human and mouse cells.

Human and mouse ARD1 proteins are degraded by different pathways during apoptosis

Previously, caspase-dependent cleavage of hARD1^{235} was reported in daunorubicin-treated HeLa cells [4]. Thus

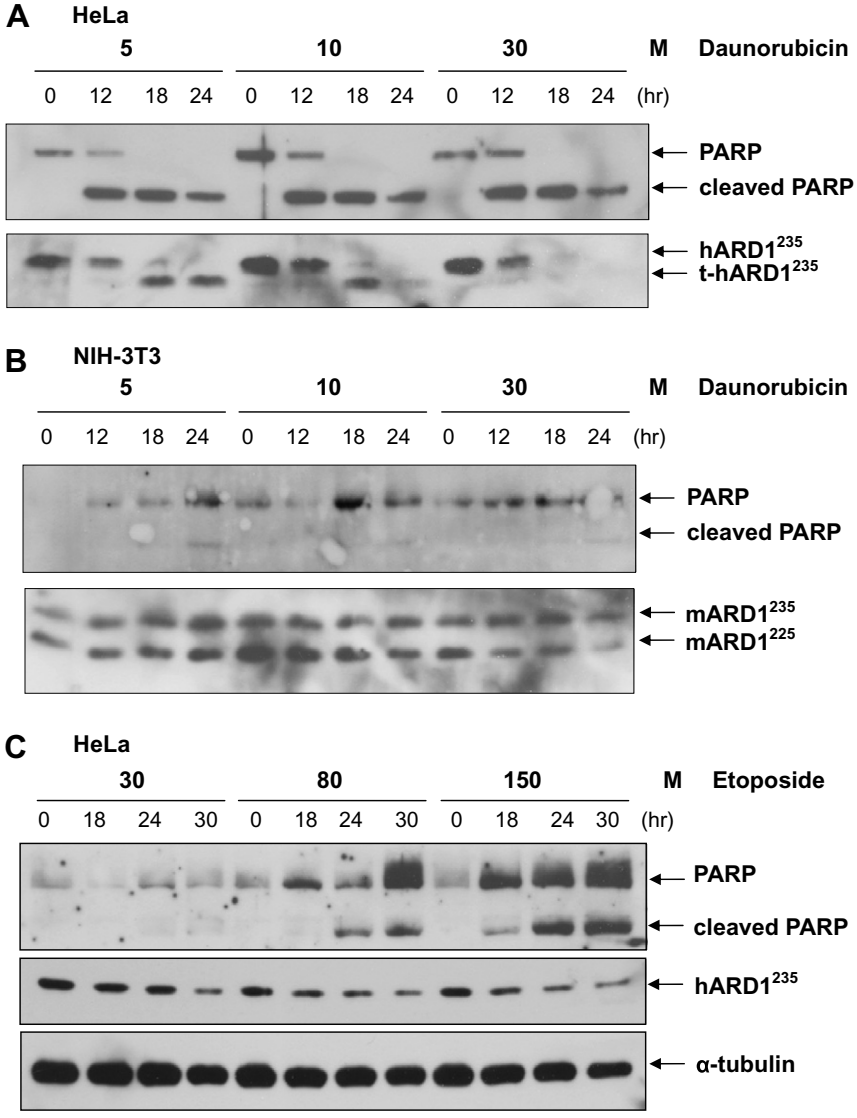

Fig. 4. ARD1 proteins are differently destabilized during apoptosis in HeLa and NIH-3T3 cells. HeLa (A) and NIH-3T3 (B) cells were treated with 5, 10 and 30 μM daunorubicin for the indicated times. Cell lysates were analyzed by immunoblotting with antibodies detecting PARP (upper panel) and ARD1 (lower panel). (C) HeLa cells were treated with 30, 80 and 150 μM etoposide for indicated times and cell lysates analyzed as above.

we asked whether mouse ARD1 proteins are also cleaved during apoptosis. As reported, truncated hARD1^{235} (t-hARD1^{235}) was detected at 18 h in cells after treatment with 10 μM daunorubicin (Fig. 4A). Cleavage of PARP served as a control for apoptosis (Fig. 4). Interestingly, we found that longer incubation with 10 μM daunorubicin resulted in degradation of t-hARD1^{235}. To determine whether mARD1^{235} and mARD1^{225} are similarly regulated during apoptosis, we treated NIH-3T3 mouse cells with daunorubicin. Although apoptosis was induced at concentrations as low as 5 μM, truncated forms of mARD1^{235} and mARD1^{225} were not detected (Fig. 4B). Instead, degradation of mARD1 proteins were observed at late time points at high doses of daunorubicin (24 h, 30 μM in Fig. 4B).

Next, to determine whether caspase-mediated cleavage of human ARD1^{235} commonly occurs during apoptosis mediated by DNA damage, we treated HeLa cells with etoposide, a well-known topoisomerase II inhibitor. Apoptosis was induced at all doses as indicated by the proteolytic cleavage of PARP (Fig. 4C). Unexpectedly, truncated form of human ARD1^{235} was not observed and only degradation was detected over time at all etoposide doses (Fig. 4C). Similarly, mARD1^{235} and mARD1^{225} were degraded at 80 and 150 μM etoposide in NIH-3T3 cells without cleavage (data not shown). These results suggest that cleavage of human ARD1^{235} is not an obligatory event in etoposide-induced DNA damage pathway and that ARD1 isoforms are degraded at late stages of apoptosis in both human and mouse cells.

Discussion

Previously, we showed that ARD1^{235} and ARD1^{225} isoforms are derived from alternative splicing at different 3′ splice sites of exon VIII [7]. Alternative splicing occurs commonly in various species, such as human, mouse, *Drosophila* and *Caenorhabditis elegans*, emphasizing the importance of alternative splicing throughout evolution [10–15]. Moreover, in this report, we show that alternative splicing of ARD1 gene is species-specific event from RT-PCR analysis, an intron/exon junction study and Western blotting. Results of a search for orthologous proteins and alignment of ARD1 genomes from the databases also support this observation. This species-specific alternative splicing between humans and mouse has been reported to be frequent events [16–18], suggesting that the diversity of a large part of the species-specific proteome is derived from alternative splicing.

In all mouse cell lines examined, ARD1^{225} transcript was more abundant than ARD1^{235} transcript. One possible explanation for this is that the alternative 3′ splice site of the intron adjacent to exon VIIIb (GTCCCTTCCCCCAG) has a more conserved string of pyrimidines (underlined) and can be easily attacked at the branch point than that of exon VIIIa (GCTCCTGGCGGCAG) during the splicing event.

Previously, it was suggested that caspase-mediated cleavage of hARD1^{235} may occur at Asp223 (EST**D**) and Asp226 (DVK**D**) during apoptosis [4]. Interestingly, we observed that human ARD1^{235} was cleaved after PARP cleavage induced by caspase-3 in daunorubicin-treated HeLa cells (Fig. 4A), indicating that hARD1^{235} may be cleaved by a protease downstream of caspase-3. This hypothesis is supported by the fact that etoposide, which also activates caspase-3 in HeLa cells, induced PARP cleavage but did not induce ARD1^{235} cleavage (Fig. 4C). Moreover, ARD1^{235} cleavage was not detected in daunorubicin-treated NIH-3T3 cells (Fig. 4B), although putative caspase-mediated cleavage sites are conserved in mouse ARD1^{235}. Therefore, further studies are necessary to elucidate protease required for the cleavage of ARD1 proteins during apoptosis.

The amino acids composition of two isoforms differs somewhat: the C-terminus of ARD1^{235} is more hydrophilic (with 23.1% acidic residues) than that of ARD1^{225} (with 8.9% acidic residues) (from aa 158). In mouse cells, the mARD1^{235} isoform was primarily nuclear, while mARD1^{225} was mostly cytoplasmic (Fig. 3). Differences in subcellular localization of these two isoforms are, at least, possibly correlated with changes in protein structure. Also, it is possible that mARD1^{225} may function differently from nuclear mARD1^{235} in mouse cells. Further study is required to determine whether hydrophobicity differences between the ARD1^{235} and ARD1^{225} C-termini can influence properties, such as subcellular localization, enzyme activity, and protein stability.

Acknowledgments

This work was supported by National Research Laboratory Fund (M10104000129-02J0000-05910) (to S.-K.L.) and the Creative Research Initiatives (to K.-W.K.) of MOST/KOSEF, Korea.

Appendix A. Supplementary data

Supplementary data associated with this article can be found, in the online version, at doi:10.1016/j.bbrc.2006.11.131.

References

[1] M. Fu, C. Wang, J. Wang, B.T. Zafonte, M.P. Lisanti, R.G. Pestell, Acetylation in hormone signaling and the cell cycle, Cytokine Growth Factor Rev. 13 (2002) 259–276.
[2] U. Mahlknecht, D. Hoelzer, Histone acetylation modifiers in the pathogenesis of malignant disease, Mol. Med. 6 (2000) 623–644.
[3] M. Whiteway, J.W. Szostak, The ARD1 gene of yeast functions in the switch between the mitotic cell cycle and alternative developmental pathways, Cell 43 (1985) 483–492.
[4] T. Arnesen, D. Anderson, C. Baldersheim, M. Lanotte, J.E. Varhaug, J.R. Lillehaug, Identification and characterization of the human ARD1-NATH protein acetyltransferase complex, Biochem J. 386 (2005) 433–443.

[5] N. Sugiura, S.M. Adams, R.A. Corriveau, An evolutionarily conserved N-terminal acetyltransferase complex associated with neuronal development, J. Biol. Chem. 278 (2003) 40113–40120.
[6] J.W. Jeong, M.K. Bae, M.Y. Ahn, S.H. Kim, T.K. Sohn, M.H. Bae, M.A. Yoo, E.J. Song, K.J. Lee, K.W. Kim, Regulation and destabilization of HIF-1alpha by ARD1-mediated acetylation, Cell 111 (2002) 709–720.
[7] S.H. Kim, J.A. Park, J.H. Kim, J.W. Lee, J.H. Seo, B.K. Jung, K.H. Chun, J.W. Jeong, M.K. Bae, K.W. Kim, Characterization of ARD1 variants in mammalian cells, Biochem. Biophys. Res. Commun. 340 (2006) 422–427.
[8] R. Bilton, N. Mazure, E. Trottier, M. Hattab, M.A. Dery, D.E. Richard, J. Pouyssegur, M.C. Brahimi-Horn, Arrest-defective-1 protein, an acetyltransferase, does not alter stability of hypoxia-inducible factor (HIF)-1alpha and is not induced by hypoxia or HIF, J. Biol. Chem. 280 (2005) 31132–31140.
[9] A. Siepel, G. Bejerano, J.S. Pedersen, A.S. Hinrichs, M. Hou, K. Rosenbloom, H. Clawson, J. Spieth, L.W. Hillier, S. Richards, G.M. Weinstock, R.K. Wilson, R.A. Gibbs, W.J. Kent, W. Miller, D. Haussler, Evolutionarily conserved elements in vertebrate, insect, worm, and yeast genomes, Genome Res. 15 (2005) 1034–1050.
[10] D. Brett, H. Pospisil, J. Valcarcel, J. Reich, P. Bork, Alternative splicing and genome complexity, Nat. Genet. 30 (2002) 29–30.
[11] A.A. Mironov, J.W. Fickett, M.S. Gelfand, Frequent alternative splicing of human genes, Genome Res. 9 (1999) 1288–1293.
[12] D. Brett, J. Hanke, G. Lehmann, S. Haase, S. Delbruck, S. Krueger, J. Reich, P. Bork, EST comparison indicates 38% of human mRNAs contain possible alternative splice forms, FEBS Lett. 474 (2000) 83–86.
[13] Z. Kan, E.C. Rouchka, W.R. Gish, D.J. States, Gene structure prediction and alternative splicing analysis using genomically aligned ESTs, Genome Res. 11 (2001) 889–900.
[14] B. Modrek, A. Resch, C. Grasso, C. Lee, Genome-wide detection of alternative splicing in expressed sequences of human genes, Nucleic Acids Res. 29 (2001) 2850–2859.
[15] J.M. Johnson, J. Castle, P. Garrett-Engele, Z. Kan, P.M. Loerch, C.D. Armour, R. Santos, E.E. Schadt, R. Stoughton, D.D. Shoemaker, Genome-wide survey of human alternative pre-mRNA splicing with exon junction microarrays, Science 302 (2003) 2141–2144.
[16] R.N. Nurtdinov, Artamonova II, A.A. Mironov, M.S. Gelfand, Low conservation of alternative splicing patterns in the human and mouse genomes, Hum. Mol. Genet. 12 (2003) 1313–1320.
[17] Q. Pan, M.A. Bakowski, Q. Morris, W. Zhang, B.J. Frey, T.R. Hughes, B.J. Blencowe, Alternative splicing of conserved exons is frequently species-specific in human and mouse, Trends Genet. 21 (2005) 73–77.
[18] H. Nagasaki, M. Arita, T. Nishizawa, M. Suwa, O. Gotoh, Species-specific variation of alternative splicing and transcriptional initiation in six eukaryotes, Gene 364 (2005) 53–62.